

## UNDERSTANDING FORMS BY MAN AND COMPUTER USING COMPUTER GRAPHICS AND IMAGE PROCESSING

Jun-ichiro TORIWAKI, Hiroshi OHSHITA, and Toyofumi SAITO

*Department of Information Engineering, Faculty of Engineering, Nagoya University,  
Furo-cho, Chikusa-ku, Nagoya 464-01, Japan*

Key words: 3D image, 3D curve, Digital topology, MRI heart image

**Abstract.** In this paper we present two topics from our research activities concerning morphological information processing. One is the recognition of the form of a 3-D closed curve. If a 2-D picture of 3-D curves drawn according to certain rules is given, one of basic problems in understanding such picture is to determine whether those curves are knotted, unknotted, linked or unlinked. An algorithm is shown to reduce a given digitized 3-D curve to a simpler form and to determine whether it is knotted or not. The other is the analysis of heart movement through generating 3-D moving images of heart. First, borders of cross section of heart wall are extracted from an MRI slice sequence by thresholding and manual correction. Next, a 3-D volume of heart wall is constructed by the border sweeping method. Third, the generated 3-D heart wall is displayed by the conventional shading and rendering algorithms. From the viewpoint of morphological information processing, this part relates to manipulate (understand) the form contained in the object movement.

### 1. INTRODUCTION

Rapid progress in imaging technologies has made it much more easier to obtain a three-dimensional (3D) digitized image data. In the medical field, for example, large volume of CT and MRI images are generated every day to be diagnosed by doctors. If a stack of sectional images (slices) cutting objects in parallel is given, 3D distribution of physical characteristic values or 3D shapes of organs may be observed and analyzed by human observer and/or computer. It is not an easy work for a human observer, however, to understand 3D information exactly from a 2D image sequence. Effective use of computer graphics will be a key to solve the problem. In principle, computer may be able to interpret or measure 3D information more easily than we do since it can access 3D image data directly without passing through the intermediate stage of 2D image processing. However, 3D image

understanding by computer itself is still in the developing stage. Thus we need to develop and accumulate methods applicable to individual problems of 3D image processing. In this paper we present two examples of such basic studies relating to morphology, or shape understanding in the 3D space. First is the analysis of 3D linear closed curves. This is primarily concerning the topology of 3D digitized figures. We propose an algorithm to determine unknottedness of a 3D closed curve, and present a few properties of algorithms. Second is the processing of heart images obtained by MRI image sequences. This part mainly discusses use of computer graphics to display movement of heart wall by shaded 2D images.

## 2. PRELIMINARIES

### 2.1 3D digitized picture

A 3D digitized picture is given in a form of a 3D array. Each element of the array is a small cube and called a *voxel*. Every voxel has its own characteristic value (called a *density value*) of which the physical meaning differs according to individual problems. If the density value assumes only 0 or 1, the picture is said to be *binary*. Other cases are called grey pictures (or grey-tone pictures) in general. We usually observe such 3D array by looking over a sequence of parallel cross sections, displayed as 2D pictures. That is the reason why the array is called a 3D *picture*. Thus we reconstruct in our brain the 3D structure of objects from the sequence of cross sections. Computer can process the 3D array data directly without the intermediate stage of 2D image processing and reconstruction. Therefore it might be possible that computer surpasses human brain in 3D image analysis and in particular 3D measurement (Fig. 1).

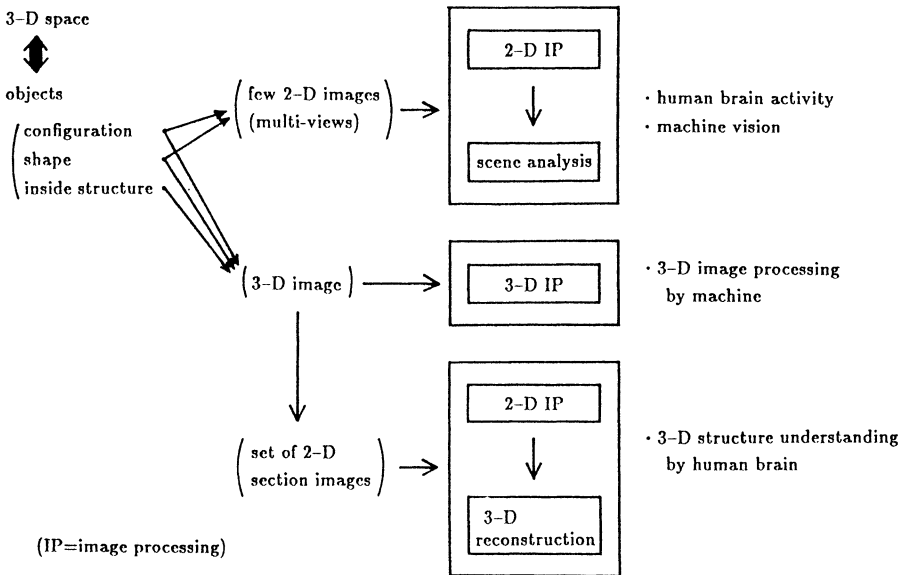


Fig. 1. 3-D image processing by human brain and machine.

## 2.2 Terminologies in digital geometry

Let us consider a binary picture  $F = \{f_{ijk}\}$ , where  $f_{ijk}$  is the density value of the voxel in the  $i$ th row and the  $j$ th column of the  $k$ th plane. Then a set of voxels

$$N^{(26)}(i, j, k) = \{(i + p, j + q, k + r); -1 \leq p, q, r \leq 1\}$$

is called the *26-neighbor* of the voxel  $P = (i, j, k)$  (Fig. 2). Any of voxels in the  $N^{(26)}(P)$  is said to be adjacent to  $P$ . A set of all 1-voxels (voxels of which density is 1) is called *figures* and that of 0-voxels the *background*. A voxel  $Q$  is said to be connected to a voxel  $P$  if  $Q$  is reached by starting from  $P$  and moving to an adjacent voxel successively. A set of 1-voxels being connected to each other is called a *connected component*, or a *figure* (Fig. 3).

A figure  $C$  with more than three voxels is called a *simple closed digital curve* (SCDC) if all 1-voxels in  $C$  have exactly two 1-voxels in their 26-neighbors (Fig. 4). SCDC is a digitized version of the simple closed curve (SCC) in geometry. It does have none of branches, thick parts, and crossing with itself or other figures.

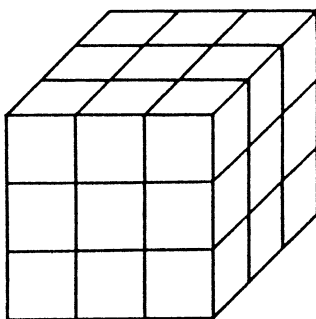
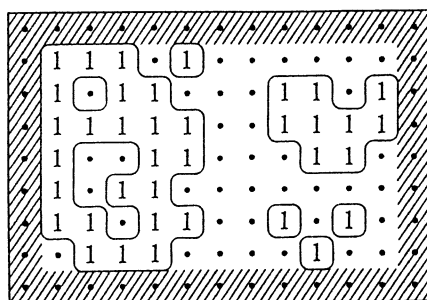


Fig. 2. 26-neighbor.



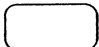
 connected component

Fig. 3. Connected components of 1-pixels in the 2-dimensional plane.

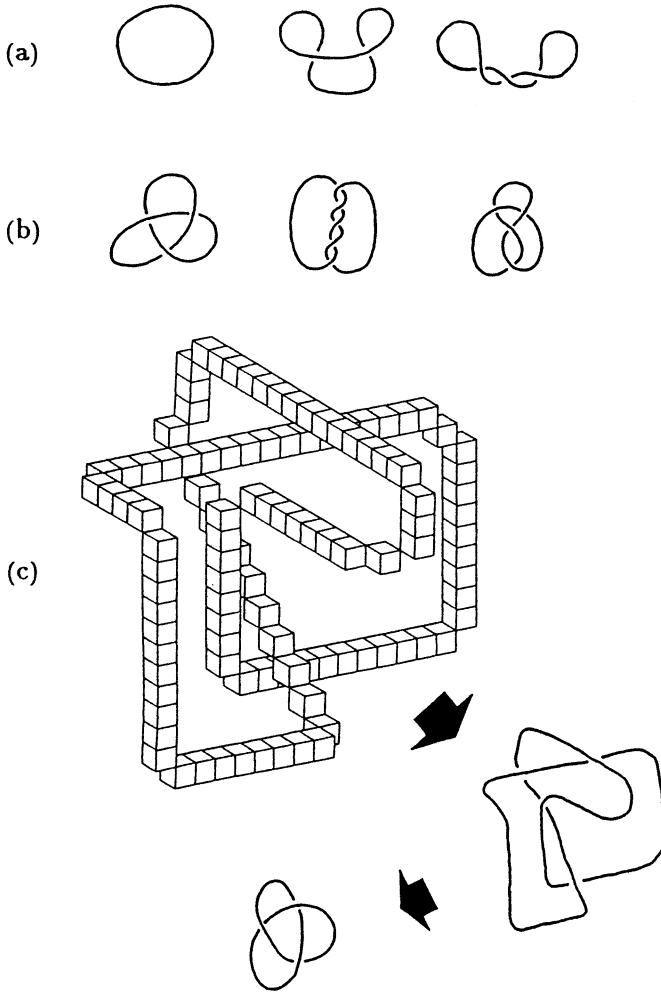


Fig. 4. Simple closed curves in the continuous 3D space ((a): unknotted, (b): knotted), and the simple closed digital curve (SCDC) in the 3D digitized space ((c): knotted).

### 3. UNDERSTANDING PROPERTIES OF LINE FIGURES

Algorithms to find the following properties have already been reported.

(1) *Connected component detection*: What we call the “labeling” is available by straightforward extension of the corresponding 2D version of the labeling procedure (Yonekura *et al.*: 1982a, Toriwaki *et al.*: 1982). The total number of components is also detected by the same procedure.

(2) *Cavity*: A *cavity* of the component  $C$  is defined as a connected component of 0-voxels which vanishes after all voxels of the component  $C$  are replaced by 0. A cavity is detected easily by inverting 0 and 1, and then applying the labeling

procedure.

(3) *Loop*: Detection of a loop in general is far more difficult than that of a connected component and a cavity (Yonekura *et al.*: 1982b, Toriwaki *et al.*: 1982, Toriwaki & Yokoi: 1983).

We present here a new result concerning detection of knottedness of an SCDC. According to the knot theory in mathematics, an SCC is classified into two types: knotted and unknotted. The knotted SCC is classified further into various types of knotting. Definition of knottedness in mathematics is defined using a 2D drawing of a 3D curve according to the specified rule (Kauffman: 1987) (Fig. 4). Instead of SCC, we consider the SCDC in the *digitized* 3D space, and derive a procedure to determine whether a given 3D SCDC is knotted or unknotted by manipulating the 3D array directly. We will define the knottedness of the SCDC in the way analogous to it in mathematics. Let us consider the center point of each 1-voxel. By connecting two such points by a straight segment if and only if corresponding two voxels are adjacent to each other, we can uniquely derive the SCC from a given SCDC. Then the knottedness of the SCDC is defined by that of the SCC obtained by the above procedure (Fig. 3).

The following results (including conjectures) have been known concerning the knottedness of an SCDC.

First, the lower limit exists in the length of the SCDC, if the length is defined by the number of voxels contained in the SCDC.

(*Property 1*) The minimum length (the number of voxels) of an unknotted SCDC is four (Fig. 5).

In fact, we cannot make a loop by three or less voxels and there is the unknotted SCDC of the length four as shown in Fig. 5.

(*Conjecture 1*) The minimum length of a knotted SCDC in the digitized 3D space is twenty-seven.

An example of the SCDC with the length 27 is already known (Fig. 6) and a smaller one has not been found yet.

(*Algorithm 1*) Let P be an arbitrary voxel on a given SCDC C.

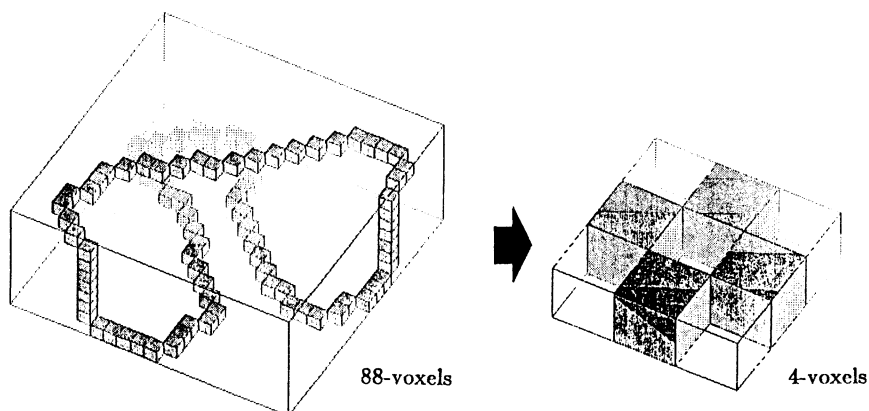


Fig. 5. The minimum unknotted SCDC.

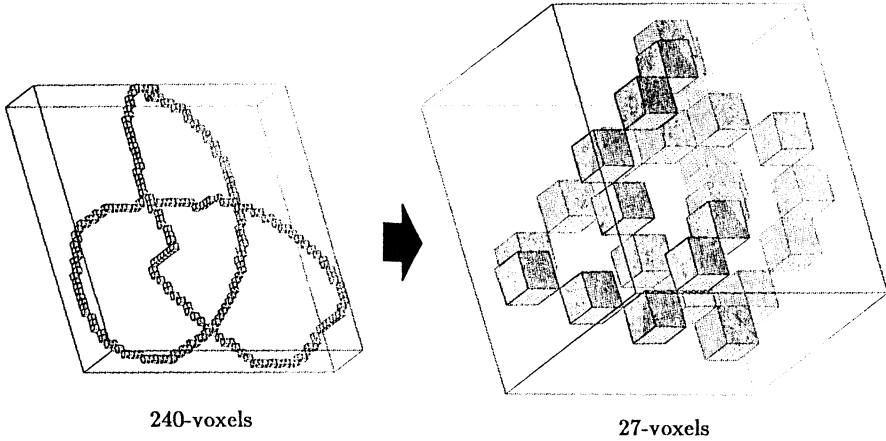


Fig. 6. An example of the knotted SCDC with 27-voxels.

- (1) Generate a straight path from P to the other voxel Q on C.
  - (2) Replace PQ by the straight line segment  $\overline{PQ}$ , if the length of the path  $\overline{PQ}$  is shorter than the arc along C between P and Q and the replacement does not cause any change in topological properties of a figure.
  - (3) Perform (2) by using all voxels of C as Q.
  - (4) Iterate (1)~(3) for all voxels of C.
  - (5) Repeat (1)~(4) until no length reduction occurs (Fig. 7).
- (Conjecture 2) By the algorithm 1, all unknotted SCDC is reduced to the one with the length 4.

It is expected that an SCDC of more complicated knottedness is reduced to the curve with the length corresponding to its complexity. In other words the length of the SCDC in the limit is used as the measure of the complexity of knottedness.

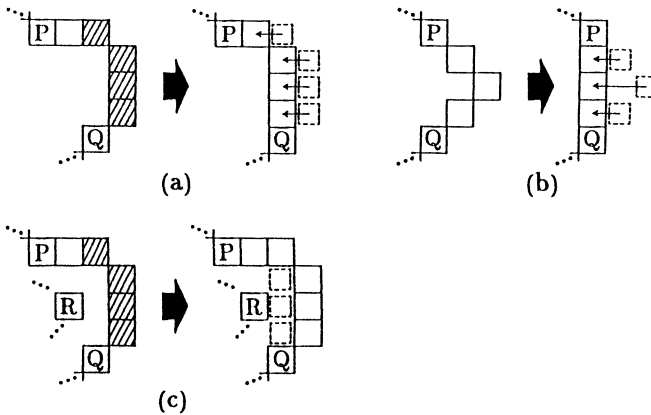


Fig. 7. Topology preserving shrinking of a SCDC ((a), (b):  $\widehat{PQ}$  is replaced by  $\overline{PQ}$ . (c): Replacement is not allowed because  $\overline{PQ}$  touches a voxel R.).

A 3D figure is obtained by imaging systems such as CT and MRI equipments in medicine. However man draws an SCC (knotted or unknotted) on a 2D plane in a particular form. Typically positional relation of two segments of a 3D curve is represented by a small gap inserted on a branch further from a viewer (Fig. 8). Therefore, computer has to understand this form of drawings to accept (input) a 3D arbitrary curve written on a paper. We developed an input software to do this work so that we may generate an arbitrarily complicated knotted curve in a 3D array stored on the computer memory. By combining this program and the procedures mentioned above we expect to implement the system to understand a picture of knotted curves.

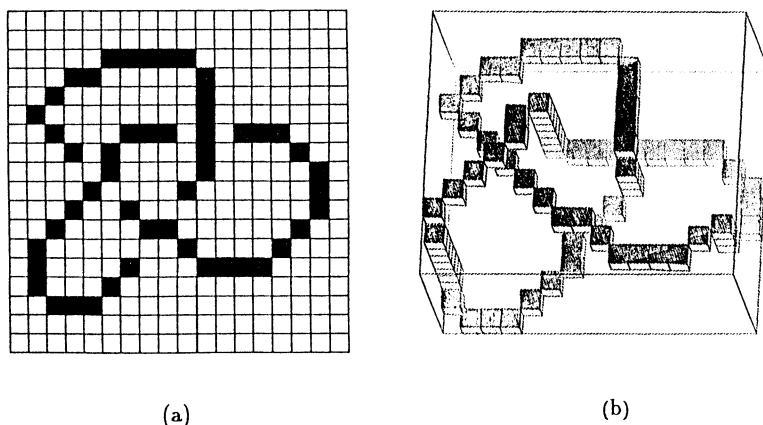


Fig. 8. Interpretation of an SCDC drawn on a 2-dimensional plane. ((a): Line drawing representing a knotted SCC after digitization and thinning. (b): 3-D SCDC generated from (a) by computer.)

## 4. UNDERSTANDING HEART MOVEMENT

### 4.1 Background

Recent MRI technology made it possible to get time sequence of sectional images of heart although temporal and spatial resolution are not always enough. Difficulty in processing such pictures is two-fold; that is, (1) reconstruction of 3D grey-tone images is required, and (2) dynamics or 3D movement of the object must be understood correctly.

The main objective here are; (1) to help human observers to understand such information, and (2) to measure features which may be important for diagnosis. Both of them will be more suitable for machine processing than manual procedures.

### 4.2 Image processing procedure

Image processing procedures we use here are as follows (Fig. 9).

(1) *Segmentation.* The heart image is extracted from each slice of MRI by the interactive thresholding and border following.

(a) Binarization of a slice is performed by changing a threshold value itera-

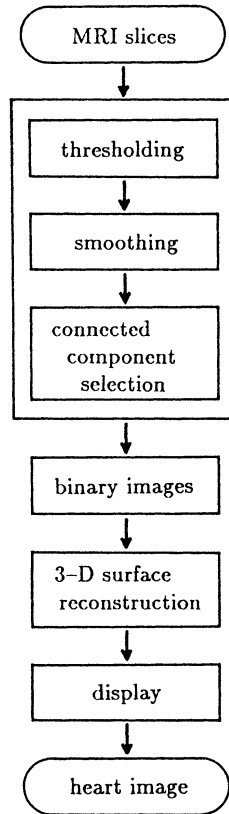


Fig. 9. Processing flow of MRI slices of heart.

tively. Extracted region is shown on a display, being overlapped on the original slice. A user selects the optimum threshold value by examining the result on a display. Three successive slices including the previous and the next slice are displayed so that the optimum threshold may be found with small numbers of iterations.

(b) Extracted heart wall regions are smoothed by the fusion (contraction–expansion) operation and the moving average of their borders.

(c) If necessary, parts of spurious regions are eliminated and a connected component is splitted into smaller pieces.

(2) *3D surface reconstruction.* Since the interval between slices is (almost six times) larger compared to the spatial resolution, we need to interpolate slices. We used the spline interpolation for the heart wall regions extracted by the above procedure. In this application we employed voxel representation of a 3D surface, and the display technique we have developed for rendering the skull image in our surgical operation simulation system NUCSS (Yasuda *et al.*: 1988, Yokoi *et al.*: 1987).



### 4.3 Experiments

Original images are a set of seventeen slices taken by the MRI system (manufactured by Siemens, with the magnetic field strength of 1.5T) and having the following specifications (Fig. 10):

voxel:  $256 \times 256$  in a slice

resolution: 9/7 mm in a slice, and 9 mm in thickness

number of slices: 17

number of phases: 13 points in one heart beat period (gated by ECG).

Examples of displayed images are shown in Fig. 11. Heart wall motion is observed by recording these images in the video tape frame by frame, and playing back them on the VTR display.

Most important advantage of this procedure is to see the heart wall motion from an arbitrary viewpoint. For example, the movement of a very particular part of the heart structure can be examined by eliminating parts of the heart occluding the region of interest and displaying the remaining parts in the way most suitable to see the parts of interest. Thus the system and the software we showed here may become a new powerful tool to understand morphological information carried by the heart dynamics.

The quality of a displayed image primarily depends on the quality of original MRI images. Those we used here seem to be the best available at present. The quality of reconstructed images is rather good in the case of static ones, but much room to be improved still remains in moving imagery.

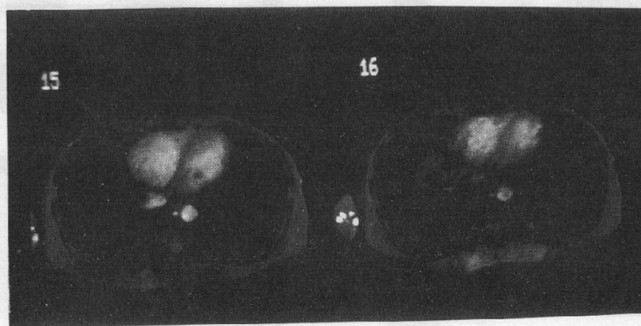


Fig. 10. Examples of slices on a graphic terminal. Extracted heart images are enhanced.

## 5. CONCLUSION

In the paper we presented two topics concerning morphological information processing from recent research activities in the authors' laboratory. One is the recognition of a form of a 3-D closed curve, and the other is the analysis of heart movement through generating 3-D images of heart. Two topics are presently not related so much explicitly. In fact they make remarkable contrast in several viewpoints such as theoretical (or fundamental)-practical (application oriented),

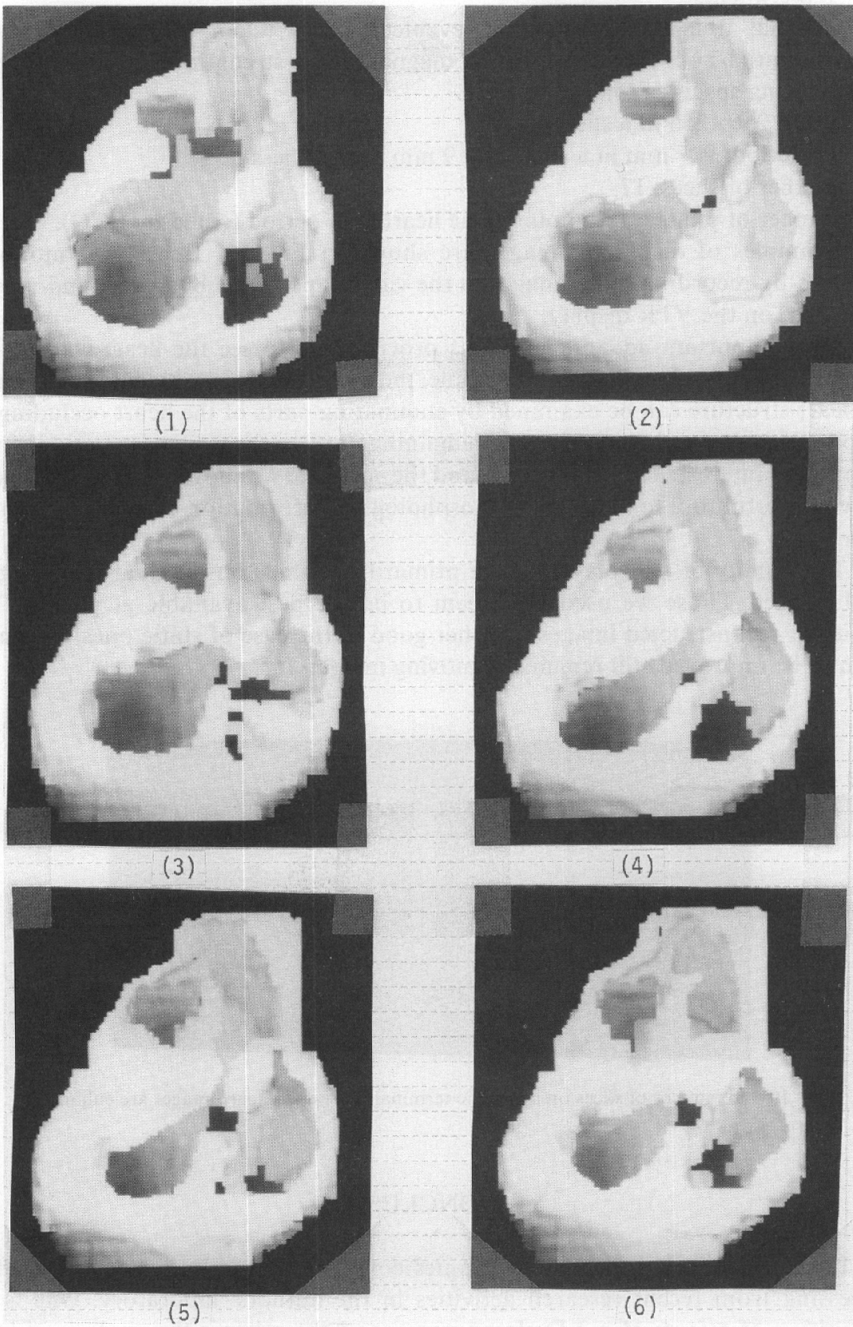


Fig. 11. Sequence of reconstructed 3-D heart images. (Numbers show time sequence)

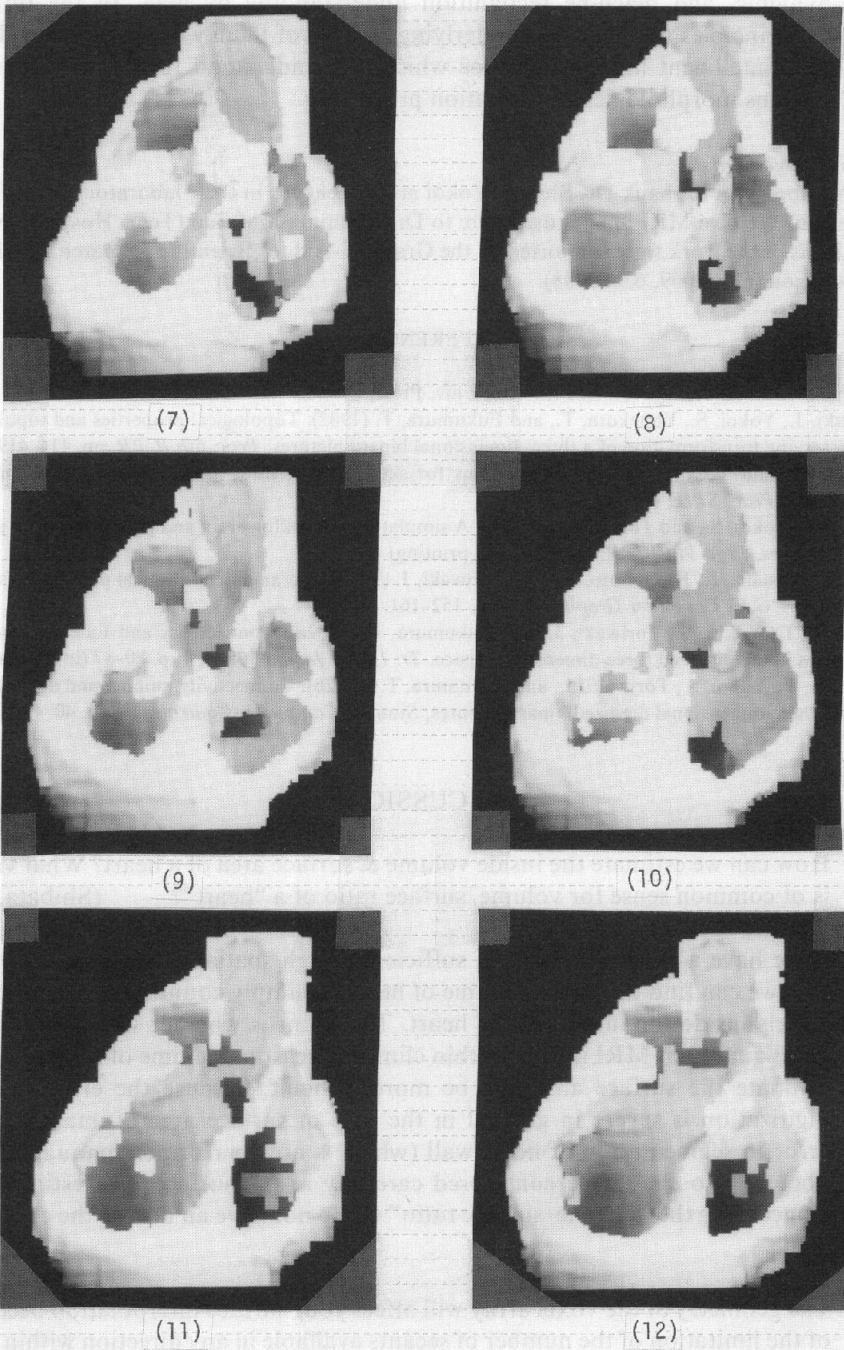


Fig. 11. (Continued).

static-dynamic, and machine recognition–understanding by man. In the future, however, principles and methods underlying in both of them will be unified to lead to flexible intelligent human interface which can understand forms by itself and assist humans morphological information processing.

#### *Acknowledgements*

Authors wish to thank Dr. Shigeki Yokoi and colleagues in their laboratory for helpful discussion. We owe MRI images used here to Dr. Michimasa Matuo (Tenri Hospital, Nara city). Parts of the work were supported by the Grant-in -Aid for Scientific Research, Ministry of Education (63633009, 63880008).

#### REFERENCES

- Kauffman, L. H. (1987): *On Knots*. Princeton Univ. Press, U.S.A.
- Toriwaki, J., Yokoi, S., Yonekura, T., and Fukumura, T. (1982): Topological properties and topology-preserving transformation of a three-dimensional binary pictures. *Proc. 6th ICPR*, pp. 414–419.
- Toriwaki, J. and Yokoi, S. (1983): Algorithms for skeletonizing three-dimensional digitized binary pictures. *Proc. SPIE*, **435**, pp. 2–9.
- Yasuda, T., Yokoi, S., and Toriwaki, J. (1988): A simulation system for brain and plastic surgeries using CT images. *Proc. 9th ICPR*, (1988–11) (In printing).
- Yokoi, S., Yasuda, T., Hashimoto, Y., and Toriwaki, J. (1987): A craniofacial surgical planning system. *Proc. NCGA's Computer Graphics '87*, pp. 152–161.
- Yonekura, T., Yokoi, S., Toriwaki, J., and Fukumura, T. (1982a): Connectivity and Euler number of figures in the digitized three-dimensional space. *Tr. IECE, Japan*, J65-D, 1, p. 80–87 (in Japanese).
- Yonekura, T., Yokoi, S., Toriwaki, J., and Fukumura, T. (1982b): Connectivity number and deletability of a three-dimensional digitized binary pictures, *Systems-Computers-Controls*, **13**, pp. 40–48.

#### DISCUSSION

- Q. How can we estimate the inside volume & surface area of a heart? What value is of common sense for volume/surface ratio of a “heart”? (Shibata, T.)
- A. If we have a 3D image data of sufficiently high spatial resolution, we think that we can find the inside volume of heart by simply counting the number of voxels inside the inner wall of heart. The point is whether we can get such good quality of MRI images within clinically reasonable time of scanning. To estimate the surface area will be more difficult, because the error due to digitization is severe in general in the case of surface area estimation. The error in segmentation of heart wall (which is now performed manually by a doctor) also should be considered carefully in the surface area estimation. Concerning the “volume/surface ratio” we do not have an idea of the concrete value.
- Q. The geometry of the voxel array will affect your surface interpolation because of the limitation of the number of secants available in any direction within any particular range of voxels. How do you deal with this? In general any estimates of volume will be reasonable while estimates of surface will invariably be less than the actual value. (Howard, C. V.)

- A. We do not have concrete (numerical) data on the error caused by the limitation of the voxel size or the way of voxel arrangement. The voxel arrangement is specified primarily by a CAT scan system. Our main concern in the present study is to what extent we can understand heart movement and how to do it. We are feeling that the spatial and the temporal resolution of the MRI available now are still not high enough for quantitative analysis of the heart function.
- Q. Do all curves of a certain knottedness reduce to the same minimum length (independent of starting configuration) and if not, do the possible minimum lengths for various degrees of knottedness overlap? (Brakenhoff, G. J.)
- A. At present, this algorithm cannot always reduce all of a certain knottedness curves to the same minimum length. According to our experimental results, lengths of reduced curves from the simplest type of knotted curves distribute over the range between 26 and 32. (A very recent result showed the minimum length of 26 which was the minimum we had found experimentally.) We are now improving the algorithms, and also are developing another algorithm based upon different types of transformations. They are now providing much better results although the unique shrinking is not guaranteed theoretically.